NASA Technical Paper 1472

Chemical Kinetic Modeling of Benzene and Toluene Oxidation Behind Shock Waves

Allen G. McLain, Casimir J. Jachimowski,
and Charles H. Wilson

AUGUST 1979

NASA

NASA Technical Paper 1472

Chemical Kinetic Modeling of Benzene and Toluene Oxidation Behind Shock Waves

Allen G. McLain, Casimir J. Jachimowski,
and Charles H. Wilson
Langley Research Center
Hampton, Virginia

NASA
National Aeronautics
and Space Administration

**Scientific and Technical
Information Branch**

1979

SUMMARY

The oxidation of stoichiometric mixtures of benzene and toluene behind incident shock waves was studied for a temperature range from 1700 to 2800 K and a pressure range from 1.1 to 1.7 atm. The concentrations of CO and CO_2 produced were measured as well as the product of the oxygen atom and carbon monoxide concentrations. Comparisons between the benzene experimental data and results calculated by use of a reaction mechanism published in the open literature were carried out. With some additional reactions and changes in rate constants to reflect the pressure-temperature range of the experimental data, a good agreement was achieved between computed and experimental results. A reaction mechanism was developed for toluene oxidation based on analogous rate steps from the benzene mechanism. For both benzene and toluene, the computed concentrations of CO were slightly higher than the experimentally measured data and the concentrations of CO_2 computed were slightly lower than the measured values. Induction times determined in the literature were reproduced very well by use of the reaction mechanisms developed in this paper.

Measurements of NO_x levels in an actual flame device, a jet-stirred combustor, were reproduced successfully with the reaction mechanism developed from the shock-tube experiments on toluene. These experimental measurements of NO_x levels were reproduced from a computer simulation of a jet-stirred combustor.

INTRODUCTION

With the increasing demands for products derived from crude oil, including jet fuels, it seems inevitable that future fuels (including those derived from synthetic crude oils) will contain higher percentages of aromatic compounds (ref. 1). It has been demonstrated that increased amounts of aromatic compounds in fuels can influence both the combustion characteristics and pollutant-emission characteristics of the fuel. Combustor studies with various fuels and fuel mixtures to which aromatic compounds have been added have shown that increases in aromatic content can result in increased levels of flame radiation, smoke, and nitrogen oxides (refs. 2 to 4). A fundamental problem in modeling any practical combustion system, such as an aircraft gas turbine, is to account for the combustion and pollutant-formation processes. If aromatic compounds become a significant percentage of the fuel composition, a need will arise to model the combustion of the aromatics, or at least in some manner to account for their presence in the fuel.

Even though much work has been done in the area of hydrocarbon combustion kinetics, most of the effort has focused on the combustion kinetics and mechanisms of paraffinic and unsaturated hydrocarbons, such as acetylene and ethylene. Very little research has been done to model the combustion of aromatic hydrocarbons. An understanding of the reaction processes which occur

during the combustion of aromatics is essential if models for fuels with high aromatic content are to be assembled. The purpose of this study was to develop and experimentally validate reaction mechanisms that can describe the combustion of two representative aromatic compounds - benzene and a substituted aromatic, toluene.

Most of the kinetic studies of aromatic compounds reported have concentrated on the ignition characteristics. Fujii and coworkers (refs. 5 to 7) and Miyama (refs. 8 and 9) have studied the ignition characteristics of benzene and various substituted aromatic hydrocarbons behind shock waves. Although the main interest in these studies was the measurement of the ignition characteristics, Fujii and coworkers (refs. 5 to 7) attempted to assemble a chemical kinetic mechanism that would describe the pyrolysis of benzene and the initial stages of the oxidation process. The mechanism provided a reasonable description of the ignition characteristics (ref. 7) but did not account for the subsequent oxidation of all the reaction products. One significant aspect of the proposed mechanism which provided the primary link between the pyrolysis processes and the formation of carbon monoxide was the direct attack on the phenyl radical C_6H_5 by molecular oxygen. This reaction was needed, according to Fujii, to explain the experimental results.

Results of an experimental and analytical study of benzene and toluene combustion behind shock waves over a temperature range of 1700 to 2800 K and pressures from 1.1 to 1.7 atm are presented in this paper. In this study, the concentrations of carbon monoxide, carbon dioxide, and the product of the concentration of the oxygen atom and carbon monoxide were monitored with infrared and ultraviolet detection systems. The experimental results were used to help guide the formulation of combustion mechanisms for benzene and toluene. The benzene combustion mechanism proposed by Fujii was used as a starting point in the mechanism development. The ignition-time data reported by Miyama were also used to help formulate the model.

SYMBOLS

$[CO], [CO_2]$	molar concentrations of CO and CO_2, mol/cm^3
$[O][CO]$	concentration product of atomic oxygen and carbon monoxide, $(mol/cm^3)^2$
C_{vib}	vibrational heat capacity
$h\nu$	energy of ultraviolet radiation
k	rate coefficient, s^{-1} for unimolecular reactions, $cm^3/mol\text{-}s$ for bimolecular reactions, $cm^6/mol^2\text{-}s$ for termolecular reactions
k_∞	rate coefficient at high pressure limit, s^{-1}
M	third-body collision partner

p	pressure, atm (1 atm = 101.3 kPa)
R	universal gas constant
s	number of effective oscillators
T	absolute temperature, K
T_m	temperature correction at the occurrence of the [O][CO] peak
t_i	induction time, s
$t_i[O_2]_o$	experimental correlation function for induction time (from ref. 8)
t_m	reaction time, μs
λ	collision efficiency factor

EXPERIMENTAL APPARATUS AND MEASUREMENT

All the experiments were carried out behind incident shock waves in a stainless-steel shock tube with an inside diameter of 8.9 cm. The test section was 671 cm long with an observation station located 625 cm from the diaphragm location. The test section and the monitoring-equipment arrangement are shown in reference 10. The calibration procedure for the monitoring equipment and the technique used to extract the quantitative results are also presented in reference 10, along with information as to the time response and accuracy of the measurement system. Briefly, the time constant for the infrared measurement system was about 3 μs and the time constant for the ultraviolet measurement system was about 2 μs.

The test gas mixture of toluene, oxygen, and argon was prepared by a commercial vendor. The mixture was made from research-pure grades of oxygen and argon and spectroanalyzed-grade toluene. The resulting mixture was 0.223 percent toluene, 2.220 percent oxygen, and 97.557 percent argon by volume. The mixture was drawn from the mixing bottle over the recommended pressure range and analyzed for the constancy of the toluene fraction. It was verified that the toluene mole fraction did remain constant down to the minimum recommended tank pressure.

The benzene test gas mixture was prepared on site from research-pure argon and oxygen and spectroanalyzed-grade benzene. The resulting mixture was 0.0250 percent benzene, 1.875 percent oxygen, and 97.875 percent argon by volume. The benzene fraction remained constant from the maximum tank pressure to the minimum tank pressure.

The shock tube was filled to a pressure of 40 mm of mercury with the test gases for all the experiments.

EXPERIMENTAL RESULTS AND DATA ANALYSIS

An example of the data obtained by shock heating the benzene-oxygen-argon mixture is shown in figure 1. The curves represent the oscilloscopic display

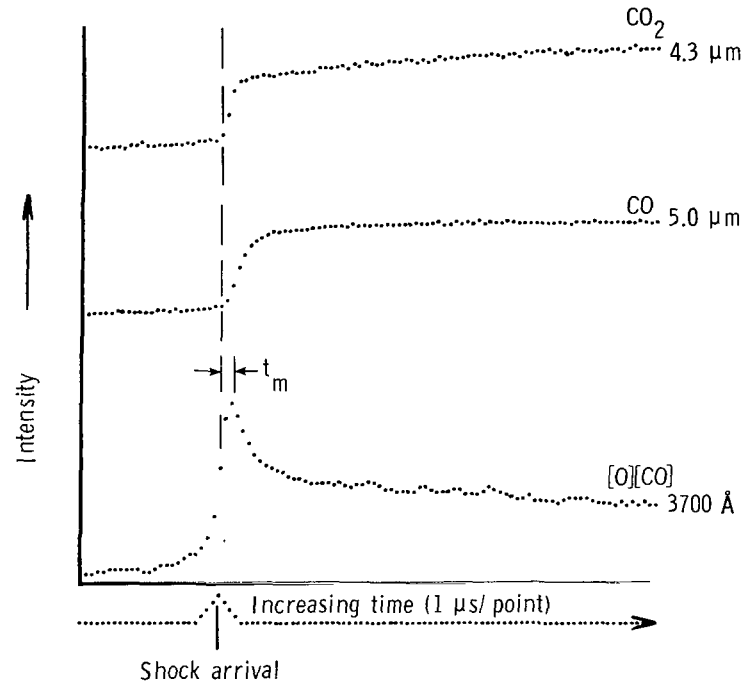

Figure 1.- Typical emission profiles for CO, CO_2, and [O][CO].

of voltage output of the [O][CO], CO, and CO_2 optical-detection equipment as changes occurred with time. The oscilloscopic displays obtained from shock heating the toluene-oxygen-argon mixture were very similar. The same features were reported in references 10 to 12 for the hydrocarbons methane, acetylene, ethylene, and propane. As with the other hydrocarbons, benzene and toluene during combustion exhibited infrared-emission profiles for CO_2 at 4.3 μm and CO at 5.0 μm. These profiles rose rapidly immediately after passage of the shock wave and then curved to an almost constant level. The emission from excited CO_2, the result of the reaction $O + CO \rightarrow CO_2 + h\nu$, was observed at a wavelength of 3700 Å. The knee of the infrared-emission profiles occurred slightly after the peak of the spike observed at 3700 Å. In most cases, the CO and CO_2 infrared-emission profiles rose quickly to an almost constant level.

The 3700-Å emission profile was analyzed by the method outlined in reference 5. The entire post-spike emission was assumed to be from the chemiluminescent reaction $O + CO \rightarrow CO_2 + h\nu$. The maximum in the emission of this reaction was assumed to occur at the same time as the maximum for the emis-

sion spike. The value at the maximum for the emission from the reaction $O + CO \rightarrow CO_2 + h\nu$ was determined by extrapolating the slope of the post-spike emission into the spike region. This value was used to calculate the concentration product [O][CO]. The values of [O][CO] calculated in this manner are shown in tables I and II.

To convert the observed infrared emissions to molar concentration units, the temperature at the maximum for the [O][CO] profile must be used. This was the approach used in references 10 to 12 to reduce the test data. The temperature predicted by the kinetic model at the peak [O][CO] value was used to extract [CO] and [CO_2] values from the calibration curves presented in reference 10. The justification for using this value T_m was presented in reference 11. The molar concentrations of CO and CO_2 are also shown in tables I and II.

COMPARISON OF THEORETICAL CALCULATIONS WITH EXPERIMENTAL RESULTS

Computer Model

The analytical model used in the parametric study involved one-dimensional flow behind an incident shock wave with finite-rate chemical reactions and boundary-layer growth. The basic computer program is described in reference 13; however, a modified form of the program described in reference 14 was used to make the calculations. This program was used to avoid time-consuming calculations caused by stiffness problems associated with systems containing many chemical species. The thermochemical data of JANAF (ref. 15) were used when given. For those compounds which had no thermochemical data in JANAF, the thermochemical data published in reference 16 were used in the curve-fitted form of reference 17.

The computer model operated in a constant-volume manner was used to simulate the conditions behind a reflected shock wave. The finite-rate chemical reaction mechanism was input for comparison with ignition-delay data available in the literature.

Proposed Reaction Mechanisms

The benzene and toluene oxidation mechanisms reported here were based, to a large extent, on the benzene pyrolysis and oxidation scheme proposed by Fujii and Asaba (refs. 5 and 6). However, additional reactions were incorporated into the benzene oxidation scheme which describe the subsequent oxidation of some pyrolysis products. Reactions analogous with the benzene mechanism were used to assemble the toluene pyrolysis and oxidation scheme.

The reaction mechanism for benzene oxidation is presented in table III and the reaction mechanism for toluene oxidation is presented in table IV. The rate coefficients listed are those which apply to the breakdown of the parent ben-

zene or toluene molecule. The reactions and rate coefficients for oxidation of the shorter-chain hydrocarbon products used in this study - methane, ethylene, and acetylene - are listed in references 11 and 12, respectively. (The methyl-radical oxidation rate coefficients appeared in the errata for ref. 12.) The reactions governing the oxidation of the parent molecule, either benzene or toluene, are discussed in the following sections. Where possible, the rate coefficients listed in references 5 and 6 were used; however, because of the differences in temperatures and pressures of this study from those in the references, a theoretical approach was used to adapt the rate coefficients to the experimental conditions.

The rate coefficients listed in tables III and IV for unimolecular reactions are the high pressure values k_∞. However, when calculations were performed at various temperatures and pressures, an adjusted rate coefficient was used. The adjusted rate coefficient was calculated from the relation $k = \frac{k}{k_\infty} k_\infty$. The ratio k/k_∞ was calculated by use of the theory of Rice-Ramsperger-Kassel (RRK) in reference 18. The use of the RRK theory requires estimates of the number of effective oscillators s and the collision efficiency factor λ. Benson (ref. 19) and Golden et al. (ref. 20) recommend that s be set equal to C_{vib}/R, where C_{vib} is the vibrational heat capacity of the reactant and R is the gas constant. The parameter λ is generally between about 0.05 and 0.9 (ref. 21), so a value of 0.1 was selected. For given values of s, λ, and k_∞, the ratio k/k_∞ was calculated by use of a method similar to the one described in reference 22.

Results of Benzene Studies

The first calculations employed the rate constants exactly as listed in references 5 and 6 to calculate the induction-time data presented in reference 8. It quickly became obvious that the rate coefficients would have to be altered to effect any reasonable comparison. Figure 2 gives the induction

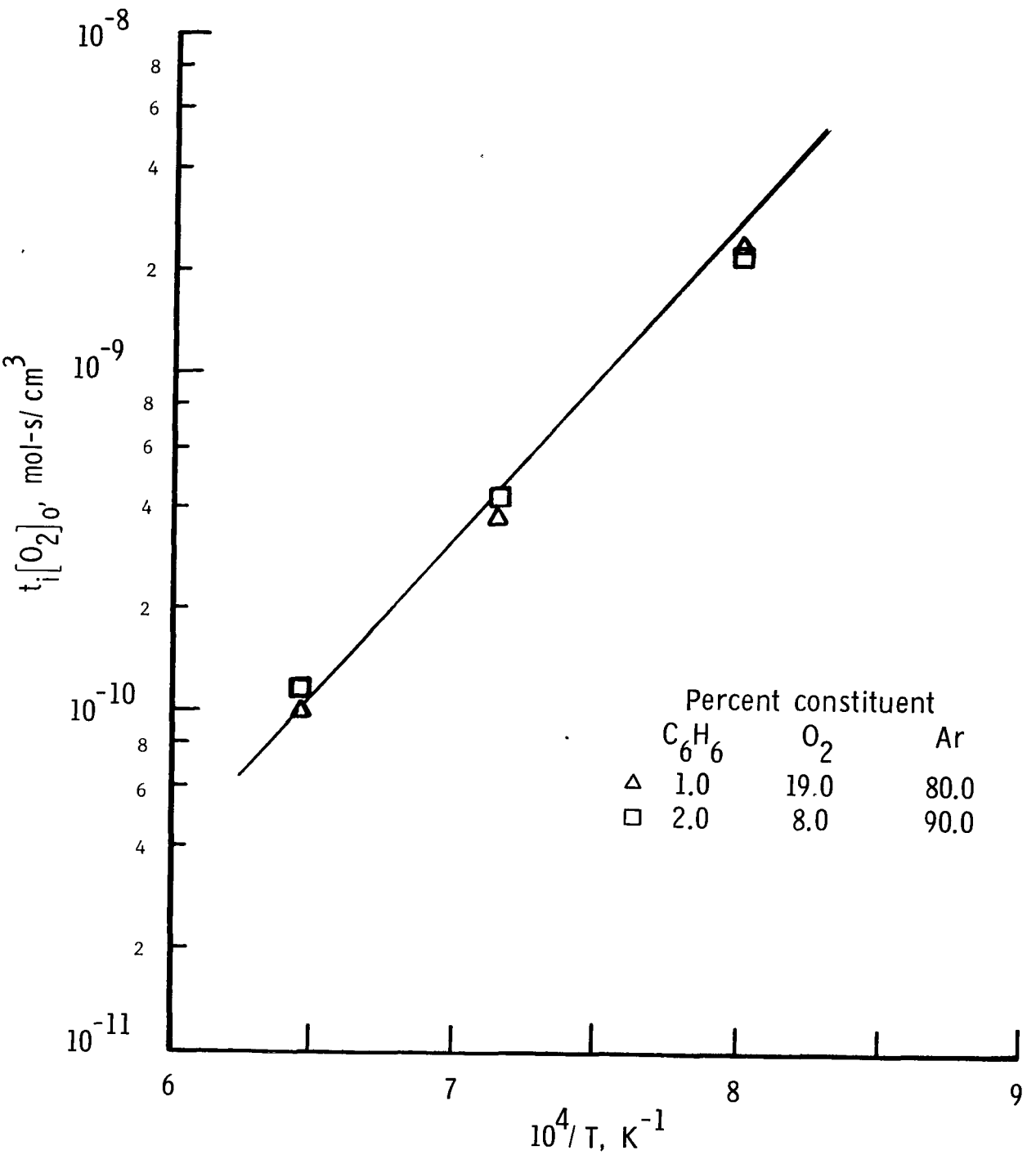

Figure 2.- Values of induction times calculated with benzene reaction mechanism (data symbols) compared with values from $t_i[O_2]_o = 1.0 \times 10^{-16} \exp 21\ 414/T$ (solid curve). Function $t_i[O_2]_o$ and benzene parameters from reference 8. Pressure, 6.0 atm.

times for benzene from reference 8 compared with the results computed by use of what was believed to be the best set of rate coefficients. Figure 3 gives

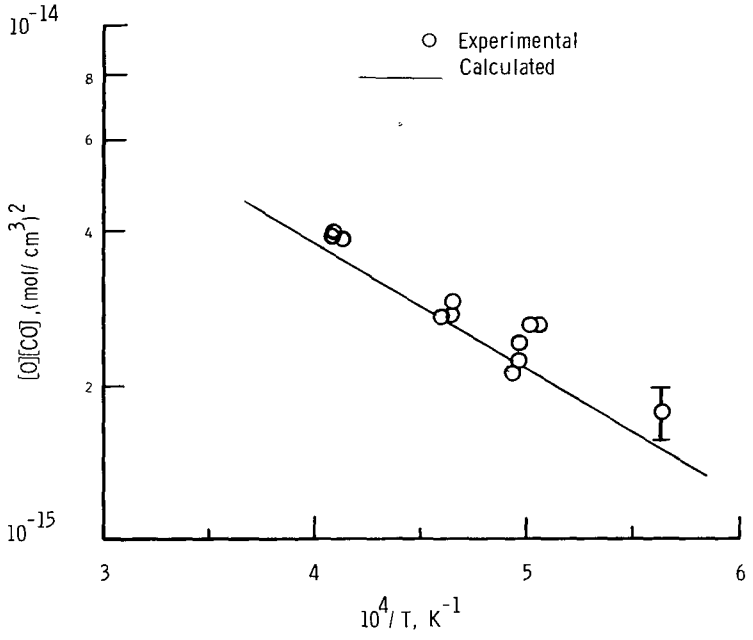

Figure 3.- Comparison of calculated and experimentally measured values of [O][CO] for combustion of benzene.

the experimental values of [O][CO] from this study and the results computed by use of the best rate-coefficient data listed in table III. The CO and CO_2 molar concentrations measured in this experimental study for the same computer simulation are shown in figure 4. The induction-time comparison was very good, as was the [O][CO] comparison. The comparison was not quite as good for [CO] and [CO_2]. The computed [CO_2] results were low by about a factor of 2, while the computed [CO] was 20 to 30 percent higher than the measured values. To achieve this comparison, the rate coefficients for reactions (3), (7), (8), (9), (10), and (11) were either altered from the values in references 5 and 6 or the reactions were added to reduce fragments of the hydrocarbon to a more reasonable final product. These reactions are discussed individually as to the reasons for the change or addition to the overall mechanism.

Reaction (3).- The rate of this reaction has a significant effect on the calculated induction times. The rate coefficient $k_3 = 4.0 \times 10^{14} \exp(-8000/RT)$, reported by Fujii and Asaba, gave induction times that were much greater than the experimental values. The expression listed in table III, together with the adjusted rate coefficient for reaction (7), gave a more reasonable description of the experimental induction times and concentrations.

Reaction (7).- The rate of this reaction has a significant effect on the calculated [CO], [CO_2], [O][CO] profiles, as well as on the induction times.

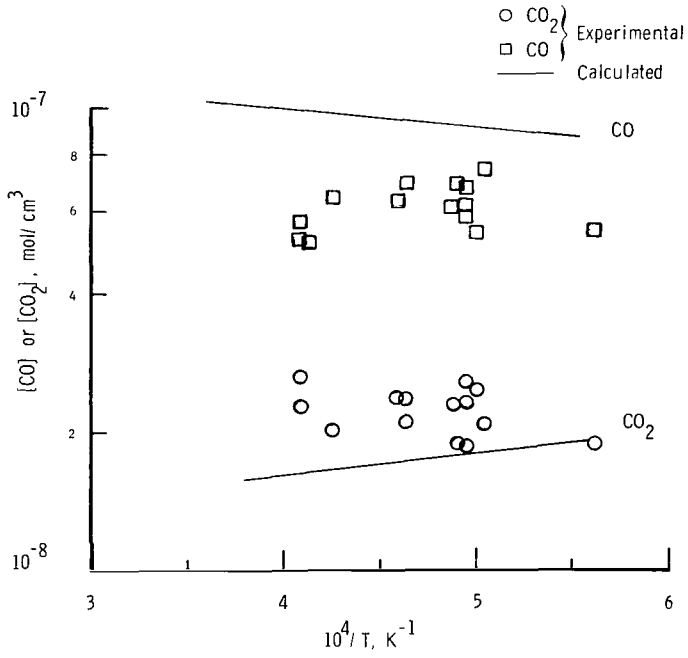

Figure 4.- Comparison of experimentally measured and calculated values of molar concentrations of CO and CO_2 from benzene combustion.

Fujii and Asaba used the rate coefficient 6.3×10^{10}. To reproduce the experimental data reported by Fujii and Asaba and the results reported here, the rate coefficient given in table III was required.

Reactions (8), (9), and (11).- The rate coefficients listed for these reactions were estimated by setting the activation energy equal to the heat of reaction ΔH at 1500 K. The preexponential factor for reactions (8), (9), and (11) was set at 10^{14} s^{-1}, which is common for the unimolecular decomposition of free radicals. (See Benson and O'Neal, ref. 23.)

Reaction (10).- This reaction describes the highly exothermic attack by atomic oxygen on diacetylene. For this reason, a preexponential factor for this reaction was assigned to be 10^{13} cm^3/mol-s with an activation energy of zero. This reaction, coupled with reaction (11), was needed to provide a reasonable reproduction of the measured [O][CO] values.

Results of Toluene Studies

The reactions needed to give reasonable comparisons with the experimental induction times and emission measurements for toluene are listed in table IV. Reactions (2), (3), and (11) are taken from references 23, 24, and 6, respectively. The reactions which are added from "Present study" are based on analogous reactions in the benzene oxidation scheme. The reaction mechanism of table IV gave good agreement for comparisons of calculated induction times with times measured experimentally in reference 8. (See fig. 5.) Reaction (8) of

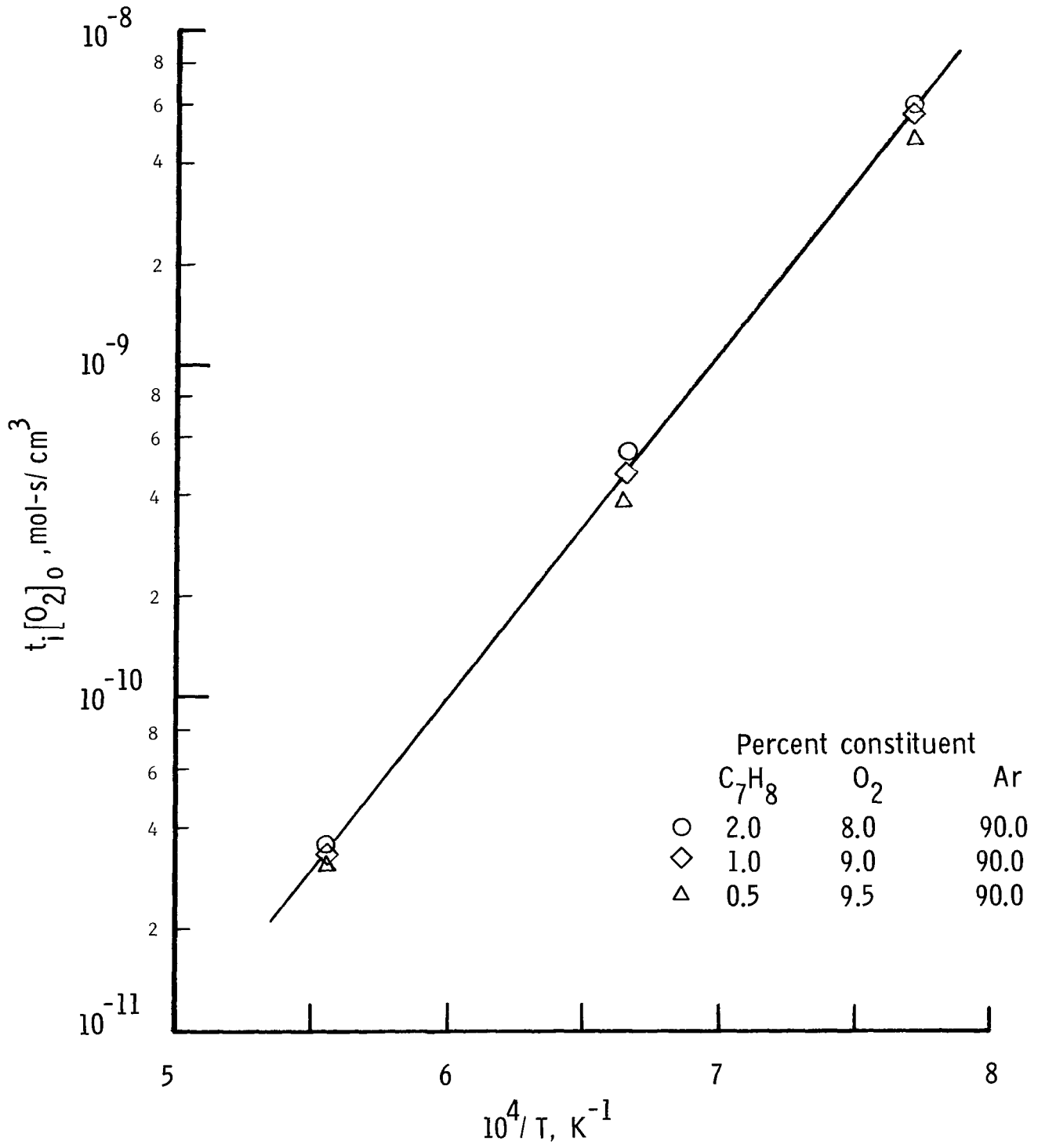

Figure 5.- Values of induction times calculated with toluene reaction mechanism (data symbols) compared with values from $t_i[O_2]_o = 6.02 \times 10^{-17} \exp 23\,855/T$ (solid curve). Function $t_i[O_2]_o$ and toluene parameters from reference 8. Pressure, 5.0 atm.

this reaction mechanism had the most effect on induction time. The comparison of calculated [O][CO] with the experimentally measured [O][CO] is shown in figure 6. Again, the agreement was very good. The CO and CO_2 molar concentra-

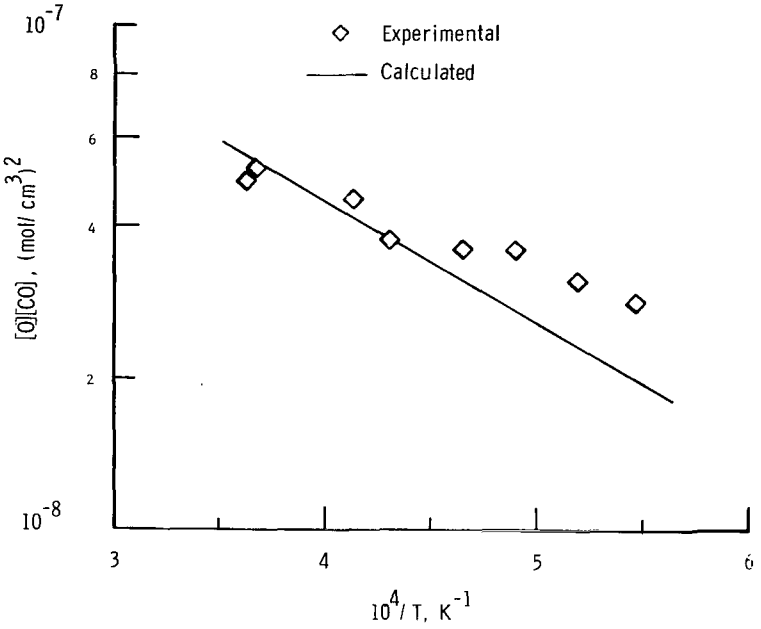

Figure 6.- Comparison of experimental and calculated values of [O][CO] from toluene combustion.

tions are shown in figure 7. Here the same deficiency in the comparison of calculated and experimentally measured results was observed for toluene as for benzene. The $[CO_2]$ calculated values were lower by almost a factor of 2 than the experimental values, and calculated [CO] was high by about 20 percent. Obviously, a reaction creating CO_2 and reducing CO is needed, but obvious reactions oxidizing CO to CO_2 do not produce the desired results. In any event, the reaction mechanism does seem to produce a reasonable description of the oxidation process. The individual reactions are discussed as to why they were selected and what effect is produced.

Reaction (1).- The rate coefficient for this reaction was estimated by setting the activation energy equal to the heat of reaction ΔH at 1500 K. The preexponential factor was set at 10^{14} cm^3/mol-s. This rate coefficient probably represents an upper limit.

Reactions (4), (5), and (6).- The rate coefficients for these reactions were estimated by use of Hirschfelder's rule (ref. 18) to determine the activation energy. The preexponential factors were set at values comparable to the preexponential factors for analogous reactions in the benzene oxidation mechanism.

Reaction (7).- This reaction describes the attack of atomic oxygen on the CH_2 group attached to the ring. Because the reaction is very exothermic,

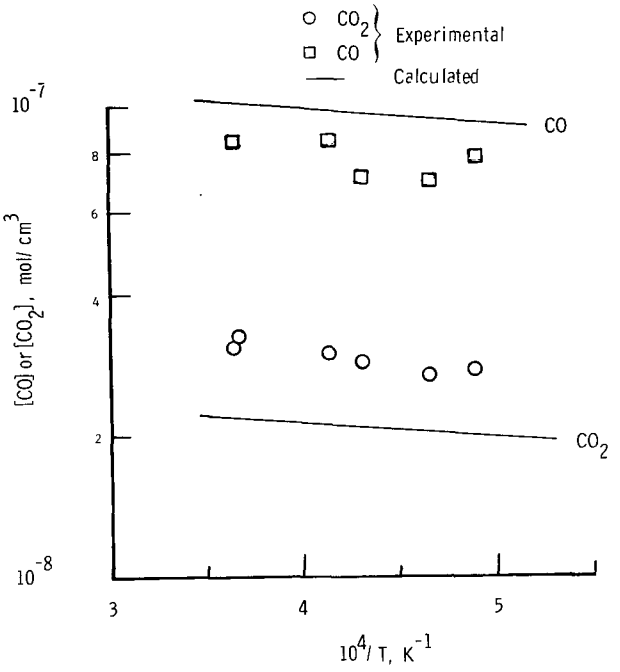

Figure 7.- Comparison of experimental and calculated values of molar concentration of CO and CO_2 from toluene combustion.

a zero activation energy was assumed. The preexponential factor was set at 10^{13} cm^3/mol-s. Subsequent parametric studies showed that a lower value of 10^{12} cm^3/mol-s did not significantly affect the calculated results.

Reaction (8).- This reaction was included in the mechanism as analogous to reaction (7) in the benzene oxidation mechanism. This reaction was needed in the mechanism to reasonably reproduce the experimental induction times. The rate coefficient listed in table IV gave the best fit between the calculated and experimental induction times.

Reactions (9), (10), (12), and (13).- These reactions describe the unimolecular decomposition of hydrocarbon radicals. The activation energies were set equal to the heat of reaction ΔH at 1500 K, and the preexponential factors were set at values comparable with those for similar reactions. (See Benson and O'Neal, ref. 23.)

Reaction (14).- This reaction is highly exothermic, and therefore an activation energy of zero was assigned. The preexponential factor was set at 1.0×10^{13} cm^3/mol-s.

The spread in reaction time measured after the passage of an incident shock wave is shown for benzene and toluene in figures 8(a) and 8(b), respectively. The band represents the uncertainty in the location of the [O] [CO] spike beneath the initial hydrocarbon spike. The spread in reaction time varies from as little as 5 μs at the high temperatures to as much as 15 μs at

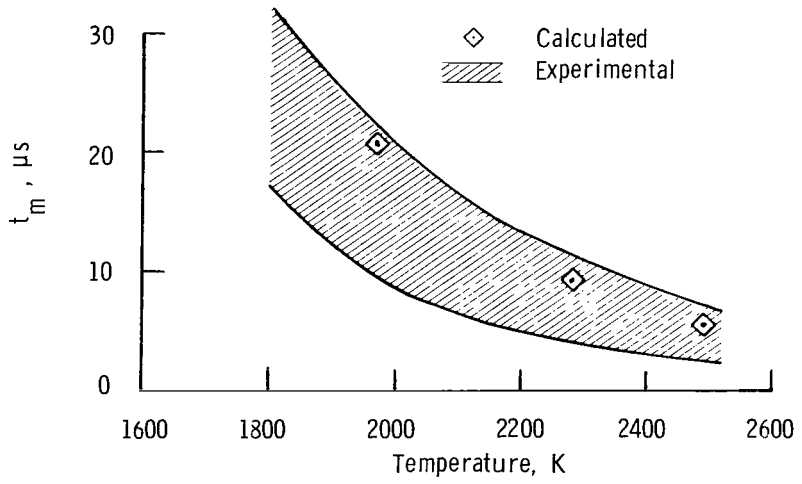

(a) Induction times for benzene.

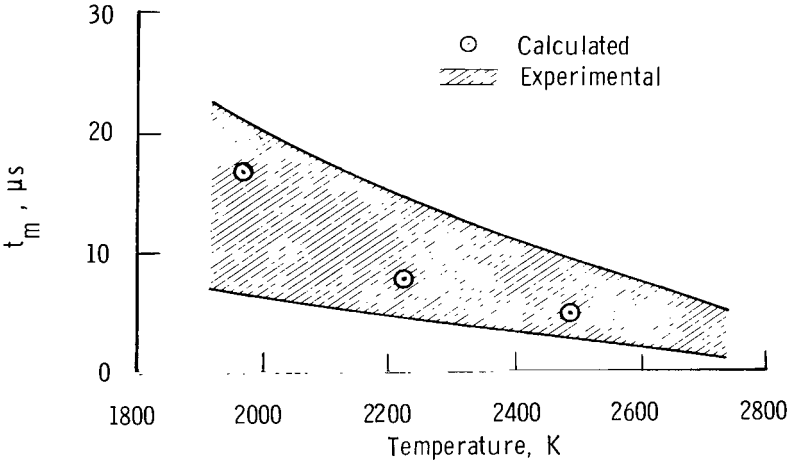

(b) Induction times for toluene.

Figure 8.- Comparison of reaction t_m time to maximum [O][CO] value for experimental and calculated cases behind incident shock waves.

the low temperatures. The symbols on the figure represent the calculated time to the peak of the [O][CO] profile. The calculated values lie within the band measured experimentally.

It was evident from viewing the oscillographic recording of the emission radiation detectors that very erratic behavior at temperatures below 1800 K occurred. This peculiarity was noted in previous studies of ethylene, acetylene, and propane, but at much lower temperatures. This behavior was observed as sharp rises and drops noted from each of the emission-radiation-detector outputs. The reason for this behavior is not known.

APPLICATION OF TOLUENE COMBUSTION MECHANISM TO STUDIES OF NITRIC OXIDE FORMATION

To assess the ability of a chemical kinetic mechanism developed from shock-tube studies to describe the combustion behavior of toluene in an actual combustion device, a comparison was made between experimentally measured nitric oxide levels and levels predicted by a model composed of the toluene oxidation mechanism reported here coupled with a reaction mechanism for nitric oxide formation. The rate of nitric oxide production during combustion is controlled not only by the flame temperature, but also by the oxygen atom concentration. The oxygen atom concentration, however, is controlled by the kinetics of the combustion process. Therefore, the ability of a model to reasonably reproduce the measured nitric oxide levels would be an indicator that the combustion mechanism provides a reasonable description of the combustion process.

The nitric oxide data that were used in the comparison were obtained from experiments with various toluene-air mixtures in the jet-stirred combustor described in reference 25. Briefly, the experimental system consisted of a cast-zirconia combustor having a spherical external geometry 1.905 cm in diameter and a hemispherical combustion cavity with a volume of 12.7 cm^3. The toluene was heated, atomized, and thoroughly mixed with heated air before being introduced into the combustor. Fuel and air flows were adjusted to achieve selected equivalence ratios within the range of 0.7 to 1.0 while maintaining a mass loading of 0.0727 $g/s\text{-}cm^3$. The fuel-air mixtures flowing into the combustor were preheated to a temperature of 455 K. The reaction pressure was 1 atm. Nitric oxide measurements were made with a chemiluminescent analyzer on a sample extracted from within the combustion cavity through a water-cooled gas-sampling probe. Gas temperatures within the combustion cavity were measured with an iridium--iridium+ 40-percent-rhodium thermocouple. Other details of the experimental system are given in reference 26. The experimental results are shown in figures 9 and 10 in which temperature and NO concentration are plotted versus the fuel-air equivalence ratio.

The reactions and rate coefficients that were combined with the toluene oxidation mechanism are listed in table V. Reactions (1') through (3') describe the formation of nitric oxide. The rate coefficients are from references 26 to 28, respectively. The recombination reactions (4') through (6') were present in the toluene mechanism; however, the rate coefficients listed in table V reflect the presence of different major third bodies M in the jet-stirred combustor experiments. The rate coefficients selected for these reactions were based on the rate coefficients reported by Jenkins et al. (ref. 29), who studied the combustion of H_2-O_2 mixtures diluted with water vapor. Jenkins performed his experiments over the temperature range 1330 to 1550 K. Since water vapor was the predominant third body, the reported rate coefficients are essentially those for $M = H_2O$. To get rate coefficients that would be applicable to the toluene-air combustor experiments, the following procedure was used.

The expressions reported by Jenkins et al. were used to calculate a rate coefficient for each reaction at the temperature 1445 K. This temperature was the average temperature in the Jenkins experiments. The temperature dependence

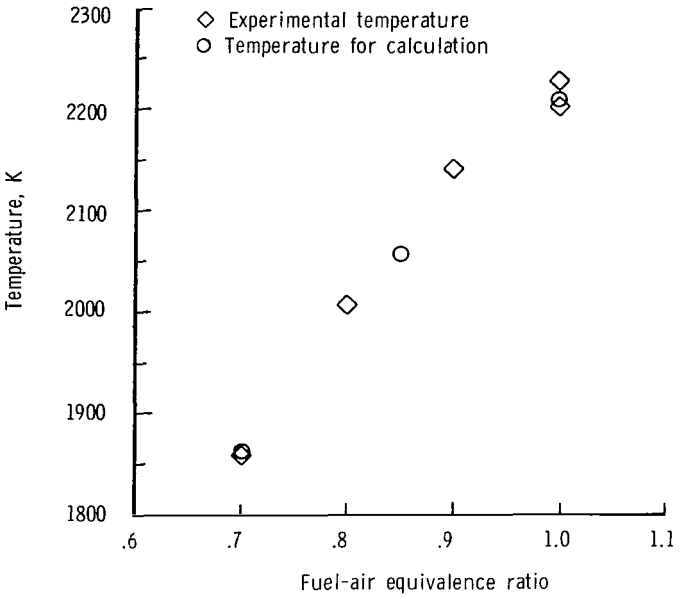

Figure 9.- Temperature of toluene-air mixtures in jet-stirred combustor.

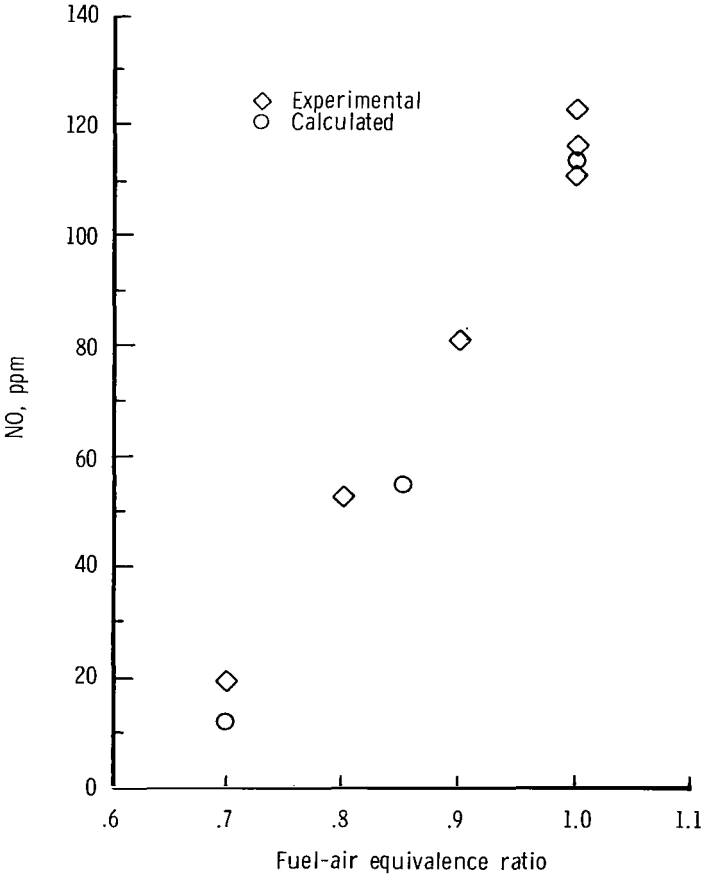

Figure 10.- Comparison between experimental and calculated nitric oxide levels in jet-stirred combustor for toluene-air mixtures.

recommended by Jensen and Jones (ref. 30) was then used to derive coefficient expressions from these rate coefficients. The resulting rate-coefficient expressions are listed in table V for $M = H_2O$. The rate-coefficient expressions for the other third bodies were assumed to be those for N_2, the predominant third body. The relative reaction efficiencies for N_2 and H_2O reported by Gay and Pratt (ref. 31) were used to obtain the $M = N_2$ rate coefficients for reactions (4') and (5'). The relative rate coefficient for reaction (6') was calculated by use of the rate coefficient at 1445 K reported by Jenkins et al. for $M = H_2O$ and the rate coefficient at 1445 K reported by Jensen and Jones for $M = N_2$.

To determine the ability of the proposed toluene combustion mechanism to predict the experimentally measured nitric oxide levels, computer simulations of the jet-stirred combustor experiments were performed with the computer program described in reference 26. These simulations were made for fuel-air equivalence ratios of 0.70, 0.85, and 1.0. The method described in reference 25 was used to match the calculated and measured temperatures. The results of these simulations are plotted in figure 10. The agreement between the measured and calculated nitric oxide levels is very good; thus the shock-tube-derived toluene mechanism provides a reasonably good description of the combustion process.

CONCLUDING REMARKS

The stoichiometric combustion of both benzene and toluene behind incident shock waves was studied over a temperature range from 1700 to 2800 K and a pressure range from 1.1 to 1.7 atm. Measurements of the concentrations of CO and CO_2 and the concentration product [O][CO] were made after the passage of the incident shock wave. A reaction mechanism of rate coefficients, taken from references when possible and calculated when no suitable rate coefficient existed, was used to effect a comparison between the measured experimental results and results from a computer model for finite-rate chemical reactions behind incident shock waves with boundary-layer growth included. Comparison was also effected between computed results and ignition-time data available in the literature. The ignition-time comparisons and the concentration product [O][CO] comparisons were very good. For both benzene and toluene, the computed [CO] and [CO_2] were off by approximately the same percentages, with computed [CO_2] lower by a factor of 2 than measured results and computed [CO] higher than measured values by about 20 percent.

The differences in the selection of rate coefficients from the literature were based on the fact that the present tests were conducted in a different temperature and pressure regime and were altered by use of the Rice-Ramsperger-Kassel (RRK) theory. Selection of necessary rate coefficients, especially for the toluene system, was based on analogous rate-coefficient steps according to the benzene system suggested in the open literature.

Several tests were run with toluene in a jet-stirred combustor and measurements of nitric oxide and temperature were made. The rate mechanism developed from the shock-tube study, with additional reactions included to describe the nitrogen chemistry, was used in a computer program which simulates

the jet-stirred combustor to calculate NO concentration and temperature. The results of the comparative test cases were very good over an equivalence-ratio range from 0.7 to 1.0 at atmospheric pressure. This demonstrates the capability of a rate mechanism developed from shock-tube results to describe the chemistry in an actual flame device - a jet-stirred combustor.

Langley Research Center
National Aeronautics and Space Administration
Hampton, VA 23665
June 12, 1979

REFERENCES

1. Longwell, J. P.: Synthetic Fuels and Combustion. Sixteenth Symposium (International) on Combustion, Combustion Inst., 1977, pp. 1-15.

2. Quigg, H. T.: Reduction of Pollutants From Aircraft Turbine by Fuel Selection and Prevaporization. Res. & Dev. Rep. 6607-73 (Contract N00140-72-C-6929), Phillips Pet. Co., Oct. 1973. (Available from DDC as AD 769 099.)

3. Schirmer, R. M.: Effect of Fuel Composition on Particulate Emissions From Gas Turbine Engines. Emissions From Continuous Combustion Systems, Walter Cornelius and William G. Agnew, eds., Plenum Press, 1972, pp. 189-210.

4. Rudey, R. A.; and Grobman, J. S.: Characteristics and Combustion of Future Hydrocarbon Fuels. NASA TM-78865, 1978.

5. Asaba, T.; and Fujii, N.: Shock-Tube Study of High-Temperature Pyrolysis of Benzene. Thirteenth Symposium (International) on Combustion, Combustion Inst., 1971, pp. 155-164.

6. Fujii, N.; and Asaba, T.: Shock-Tube Study of the Reaction of Rich Mixtures of Benzene and Oxygen. Fourteenth Symposium (International) on Combustion, Combustion Inst., 1973, pp. 433-442.

7. Fujii, N.; Asaba, T.; and Miyama, H.: Ignition of Lean Benzene Mixtures With Oxygen in Shock Waves. Acta Astronaut., vol. 1, no. 3/4, Mar./Apr. 1974, pp. 417-426.

8. Miyama, Hajime: Ignition of Aromatic Hydrocarbon-Oxygen Mixtures by Shock Waves. J. Phys. Chem., vol. 75, no. 10, 1971, pp. 1501-1504.

9. Miyama, Hajime: Ignition of Benzene-Oxygen-Argon and Benzene-Oxygen-Nitrogen Mixtures by Shock Waves. J. Chem. Phys., vol. 52, no. 7, Apr. 1970, pp. 3850-3851.

10. McLain, Allen G.; and Jachimowski Casimir J.: Chemical Kinetic Modeling of Propane Oxidation Behind Shock Waves. NASA TN D-8501, 1977.

11. Jachimowski, Casimir J.: Kinetics of Oxygen Atom Formation During the Oxidation of Methane Behind Shock Waves. Combust. & Flame, vol. 23, no. 2, Oct. 1974, pp. 233-248.

12. Jachimowski, Casimir J.: An Experimental and Analytical Study of Acetylene and Ethylene Oxidation Behind Shock Waves. Combust. & Flame, vol. 29, no. 1, May 1977, pp. 55-66. Errata in Combust. & Flame, vol. 30, no. 2, 1977, p. 102.

13. Bittker, David A.; and Scullin, Vincent J.: General Chemical Kinetics Computer Program for Static and Flow Reactions, With Application to Combustion and Shock-Tube Kinetics. NASA TN D-6586, 1972.

14. McLain, Allen G.; and Rao, C. S. R.: A Hybrid Computer Program for Rapidly Solving Flowing or Static Chemical Kinetic Problems Involving Many Chemical Species. NASA TM X-3403, 1976.

15. JANAF Thermochemical Tables - Second Edition NSRDS-NBS-37, U.S. Dep. Commer., June 1971.

16. Bahn, Gilbert S.: Approximate Thermochemical Tables for Some C-H and C-H-O Species. NASA CR-2178, 1973.

17. Wakelyn, N. T.; and McLain, Allen G.: Polynomial Coefficients of Thermochemical Data for the C-H-O-N System. NASA TM X-72657, 1975.

18. Benson, Sidney W.: The Foundations of Chemical Kinetics. McGraw-Hill Book Co., Inc., 1960, pp. 225-239 and p. 317.

19. Benson, Sidney W.: Thermochemical Kinetics. John Wiley & Sons, Inc., 1968, p. 112.

20. Golden, David M.; Solly, Richard K.; and Benson, Sidney W.: A Comparison of RRK and RRKM Theories for Thermal Unimolecular Processes. J. Phys. Chem., vol. 75, no. 10, 1971, pp. 1333-1338.

21. Troe, J.: Thermal Dissociation and Recombination of Polyatomic Molecules. Fifteenth Symposium (International) on Combustion, Combusion Inst., 1975, pp. 667-680.

22. Emanuel, George: Table of the Kassel Integral. Int. J. Chem. Kinet., vol. 4, no. 6, Nov. 1972, pp. 591-637.

23. Benson, Sidney W.; and O'Neal, H. Edward: Kinetic Data on Gas Phase Unimolecular Reactions. NSRDS-NBS 21, U.S. Dep. Commer., Feb. 1970.

24. Martinez, Maria Ramos; Miller, Donald J.; and Thommarson, Ronald L.: Automated Estimation of Kinetic Rate Parameters and Mechanisms of Complex Gas-Phase Chemical Reactions. Rep. No. MDC G5012 (Contract No. DAA D05-73-C-0503), McDonnell Douglas Astronautics Co., Jan. 1974. (Available from DDC as AD 774 304.)

25. Wakelyn, N. T.; Jachimowski, Casimir J.; and Wilson, Charles H.: Experimental and Analytical Study of Nitric Oxide Formation During Combustion of Propane in a Jet-Stirred Combustor. NASA TP-1811, 1978.

26. Blauwens, Joanna; Smets, Bruno; and Peeters, Jozef: Mechanism of "Prompt" NO Formation in Hydrocarbon Flames. Sixteenth Symposium (International). on Combustion, Combustion Inst., 1977, pp. 1055-1064.

27. Baulch, D. L.; Drysdale, D. D.; and Horne, D. G.: Evaluated Kinetic Data for High Temperature Reactions. Volume 2 - Homogeneous Gas Phase Reactions of the H_2-N_2-O_2 System. Butterworth & Co. (Publ.), Ltd., c.1973.

28. Jachimowski, Casimir J.: High-Temperature Chemical Kinetic Study of the H_2-CO-CO_2-NO Reaction System. NASA TN D-7897, 1975.

29. Jenkins, D. R.; Yumlu, V. S.; and Spaulding, D. B.: Combustion of Hydrogen and Oxygen in a Steady-Flow Adiabatic Stirred Reactor. Eleventh Symposium (International) on Combustion, Combustion Inst., 1967, pp. 779-790.

30. Jensen, D. E.; and Jones, G. A.: Reaction Rate Coefficients for Flame Calculations. Combust. & Flame, vol. 32, no. 1, 1978, pp. 1-34.

31. Gay, A.; and Pratt, N. H.: Hydrogen-Oxygen Recombination Measurements in a Shock Tube Steady Expansion. Shock Tube Research. Proceedings of the Eighth International Shock Tube Symposium, J. L. Stollery, A. G. Gaydon, and P. R. Owen, eds., Chapman and Hall Ltd., c.1971, pp. 39/1-39/13.

TABLE I.- EXPERIMENTAL RESULTS OF BENZENE COMBUSTION

T, K	p, atm	$[O][CO]$, $(mol/cm^3)^2$	$[CO_2]$, mol/cm^3	$[CO]$, mol/cm^3	T_m, K
2425	1.57	3.830×10^{-15}	----------	5.130×10^{-8}	2470
2452	1.59	3.820	2.608×10^{-8}	5.130	2505
2453	1.60	3.905	2.226	5.644	2508
2345	1.52	2.550	1.975	6.320	2406
2175	1.39	2.696	2.337	6.231	2250
2154	1.37	2.705	2.325	6.821	2229
2154	1.37	2.885	2.093	6.821	2229
2019	1.27	2.210	2.300	5.749	2105
2050	1.28	-----	2.283	6.087	2133
1996	1.25	2.589	2.442	5.342	2086
1980	1.24	2.596	2.061	7.327	2073
1780	1.09	1.750	1.866	5.373	1900
2035	1.28	2.075	1.854	6.798	2098
2020	1.27	2.394	1.839	6.740	2110
2020	1.27	2.210	2.530	6.130	2110

TABLE II.- EXPERIMENTAL RESULTS OF TOLUENE COMBUSTION

T, K	p, atm	$[O][CO]$, $(mol/cm^3)^2$	$[CO_2]$, mol/cm^3	$[CO]$, mol/cm^3	T_m, K
2730	1.80	5.190×10^{-15}	3.214×10^{-8}	8.276×10^{-8}	2794
2755	1.82	4.880	3.059	8.292	2820
2430	1.60	4.500	2.969	8.426	2499
2330	1.42	3.750	2.822	7.055	2400
2050	1.30	3.580	2.705	7.729	2135
2155	1.38	3.600	2.653	6.867	2231
1830	----	2.800	----------	----------	----
1925	----	3.100	----------	----------	----

TABLE III.- REACTION MECHANISM FOR BENZENE OXIDATION

Reaction	Rate coefficient, k (a)	Reference
(1) $C_6H_6 + O_2 \rightarrow HO_2 + C_6H_5$	6.3×10^{13} exp(-30 196/T)	6
(2) $C_6H_6 \rightarrow C_6H_5 + H$	3.2×10^{15} exp(-53 347/T)	5, 6
(3) $H + C_6H_6 \rightarrow C_6H_5 + H_2$	1.6×10^{14} exp(-4026/T)	Present study
(4) $O + C_6H_6 \rightarrow C_6H_5 + OH$	3.2×10^{14} exp(-3019/T)	6
(5) $OH + C_6H_6 \rightarrow C_6H_5 + H_2O$	1.0×10^{13} exp(-3019/T)	6
(6) $C_6H_5 \rightarrow C_4H_3 + C_2H_2$	3.2×10^{14} exp(-43 280/T)	6
(7) $O_2 + C_6H_5 \rightarrow 2\ CO + C_2H_2 + C_2H_3$	7.5×10^{13} exp(-7550/T)	Present study
(8) $C_4H_3 \rightarrow C_4H_2 + H$	1.0×10^{14} exp(-29 700/T)	Estimated
(9) $C_4H_3 \rightarrow C_2H + C_2H_2$	1.0×10^{14} exp(-29 700/T)	Estimated
(10) $O + C_4H_2 \rightarrow C_2HO + C_2H$	1.0×10^{13}	Estimated
(11) $C_2HO \rightarrow CO + CH$	1.0×10^{14} exp(-29 190/T)	Estimated

[a]The units for k are s^{-1} for unimolecular reactions, $cm^3/mol\text{-}s$ for bimolecular reactions, and $cm^6/mol^2\text{-}s$ for termolecular reactions.

TABLE IV.- REACTION MECHANISM FOR TOLUENE OXIDATION

Reaction	Rate coefficient, k (a)	Reference
(1) $C_7H_8 + O_2 \rightarrow C_7H_7 + HO_2$	1.0×10^{14} exp(-20 130/T)	Estimated
(2) $C_7H_8 \rightarrow C_7H_7 + H$	3.2×10^{15} exp(-44 440/T)	23
(3) $C_7H_8 \rightarrow C_6H_5 + CH_3$	1.0×10^{17} exp(-52 550/T)	24
(4) $H + C_7H_8 \rightarrow C_7H_7 + H_2$	1.0×10^{14} exp(-3420/T)	Estimated
(5) $O + C_7H_8 \rightarrow OH + C_7H_7$	1.0×10^{14} exp(-3625/T)	Estimated
(6) $OH + C_7H_8 \rightarrow H_2O + C_7H_7$	1.0×10^{13} exp(-1510/T)	Estimated
(7) $O + C_7H_7 \rightarrow CH_2O + C_6H_5$	1.0×10^{13}	Estimated
(8) $O_2 + C_7H_7 \rightarrow 2\ CO + C_3H_5 + C_2H_2$	5.0×10^{12} exp(-7550/T)	Present study
(9) $C_7H_7 \rightarrow C_4H_3 + C_3H_4$	1.0×10^{15} exp(-51 330/T)	Estimated
(10) $C_3H_5 \rightarrow CH_3 + C_2H_2$	1.0×10^{14} exp(-27 180/T)	Estimated
(11) $C_3H_5 \rightarrow C_3H_4 + H$	1.3×10^{13} exp(-30 790/T)	24
(12) $C_3H_4 \rightarrow CH_3 + C_2H$	1.0×10^{15} exp(-51 330/T)	Estimated
(13) $C_3H_4 \rightarrow C_2H_2 + CH_2$	1.0×10^{15} exp(-51 330/T)	Estimated
(14) $O + C_3H_4 \rightarrow C_2H_3 + HCO$	1.0×10^{13}	Estimated

[a]The units for k are s^{-1} for unimolecular reactions, $cm^3/mol\text{-}s$ for bimolecular reactions, and $cm^6/mol^2\text{-}s$ for termolecular reactions.

TABLE V.- ADDITIONAL REACTIONS NEEDED IN THE STIRRED-COMBUSTOR CALCULATIONS

Reaction	Rate coefficient, k (a)	Reference
(1') $O + N_2 \rightarrow NO + N$	$7.5 \times 10^{13} \exp(-38\ 250/T)$	26
(2') $N + O_2 \rightarrow NO + O$	$6.4 \times 10^{9}\ T^{1} \exp(-3145/T)$	27
(3') $N + OH \rightarrow NO + H$	4.0×10^{13}	28
(4') $M + 2H \rightarrow H_2 + M$:		
$M = H_2O$	$1.6 \times 10^{18}\ T^{-1}$	Estimated
$M = N_2$, all other	$2.7 \times 10^{17}\ T^{-1}$	Estimated
(5') $M + H + OH \rightarrow H_2O + M$:		
$M = H_2O$	$5.9 \times 10^{23}\ T^{-2}$	Estimated
$M = N_2$, all other	$1.2 \times 10^{23}\ T^{-2}$	Estimated
(6') $M + H + O \rightarrow OH + M$:		
$M = H_2O$	$1.6 \times 10^{20}\ T^{-1}$	Estimated
$M = N_2$, all other	$3.6 \times 10^{18}\ T^{-1}$	Estimated

[a]The units for k are s^{-1} for unimolecular reactions, $cm^3/mol\text{-}s$ for bimolecular reactions, and $cm^6/mol^2\text{-}s$ for termolecular reactions.

5 1 1U,C, 080679 S00903DS
DEPT OF THE AIR FORCE
AF WEAPONS LABORATORY
ATTN: TECHNICAL LIBRARY (SUL)
KIRTLAND AFB NM 87117